

# HIGH-TEMPERATURE DE-MOLDING FOR CYCLE TIME REDUCTION IN HOT EMBOSsing

*Matthew Dirckx<sup>1\*</sup>, Hayden K. Taylor<sup>2</sup>, and David E. Hardt<sup>1</sup>*

*<sup>1</sup>Department of Mechanical Engineering, <sup>2</sup>Department of Electrical Engineering & Computer Science,  
Massachusetts Institute of Technology, Cambridge, MA*

*\*mdirckx@mit.edu*

## Abstract

Hot micro-embossing is a promising manufacturing technique for replicating millimeter- to nanometer-scale features in thermoplastic parts. However, the thermal cycle time limits production rate, and thermal contraction mismatch between the part and the tool can lead to damage during cooling. It is thus desirable to reduce or eliminate the thermal cycle. One approach is to de-mold at higher temperature, but elastic recovery can degrade accuracy. The degree of recovery depends on processing conditions. Proper selection of these conditions permits de-molding near or above the glass transition with little or no degradation of quality.

## Introduction

Hot micro-embossing (HME), also known as micro- or nano-imprinting, has attracted increasing attention for its potential as a manufacturing technique for producing micro- to nano-meter scale features in thermoplastics. The HME process has been used to produce microfluidic devices such as a “lab on a chip” for DNA amplification [1], optical interconnects and fiber couplers [2], and a microfluidic device with integrated optical features including a dye laser, lenses, and waveguides [3].

In a conventional HME process, the thermoplastic workpiece is first heated above its glass transition temperature ( $T_g$ ). Next, the part is brought in contact with the tool and a forming pressure is applied. The pressure and temperature are maintained for a set period. The part and tool are then cooled while the pressure is maintained. When the desired de-molding temperature is reached, the part and tool are separated.

The time to heat and cool the part and tool usually dominates the overall time to produce a part. A great deal of effort has been spent in trying to reduce this time by increasing the heating and cooling rate capability of the embossing machine. This has been accomplished by employing alternative heating methods such as infrared radiation [4–6], ultrasonic vibration [7, 8], and direct heating of metal tools with high frequency electric current [9], as well as by innovative machine design [10, 11]. All of these methods have successfully reduced the processing

time in HME, but they require specially designed tools and machines, and can restrict the range of usable tool materials.

The thermal cycle also has important consequences for part quality. Various investigators have observed distortion and damage of both parts and tools, caused by differential thermal contraction between the part and the tool [12–14]. The thermal cycle inherent in conventional HME has negative consequences for both production rate and quality. It is thus desirable to reduce or eliminate any change in temperature as part of the embossing process. Yao and Nagarajan [15] embossed channel-like features into polytetrafluoroethylene at room temperature and observed good replication at very high pressures, although elastic recovery resulted in the channels being 30% narrower than the tool features. Transparent glassy polymers such as polymethylmethacrylate (PMMA), cyclo-olefin copolymer, and polycarbonate are preferred for microfluidic and micro-optical applications, and room-temperature embossing of these brittle materials may not be practical.

## High-Temperature De-molding

Although the thermal cycle time for HME has been reduced by innovative heating methods and machine design, the thermal cycle itself can cause quality problems. The most attractive materials for microfluidic and micro-optical devices are difficult to form at room temperature, so temperatures above  $T_g$  must still be used. It is possible to use a simple, conventional embossing machine and de-mold at high temperature. The part can be pre-heated before embossing and cooled separately after de-molding, potentially accelerating the production rate. Moreover, since the part would not then be in contact with the tool during cooling, thermal contraction mismatch would not be a problem.

Above  $T_g$ , amorphous polymers enter a rubbery state in which they can support large deformations and still recover to nearly their original shape. Such recovery could pose a major problem for high-temperature de-molding, since embossed features may, under certain conditions, spring back when the load is removed. It is possible, however, to exploit the time-dependent viscous behavior of the polymer to produce permanent deformation. Proper

selection of the processing parameters can permit de-molding near or above  $T_g$ , while preventing significant spring-back.

## Experimental Method

The embossing machine used in the current study has been described in detail in [16]. It consists of two copper platens heated and cooled by oil flowing through several internal passages. The oil is heated and cooled in a separate thermal control system. The platens are mounted to an Instron model 5869 load frame, which controls the embossing force and displacement. A layer of silicone rubber provides for fine alignment and ensures an even pressure distribution across the part (Figure 1).

The part material used is 1.5 mm thick Lucite CP PMMA sheet. This material has a 1.8 MPa heat deflection temperature of 90 °C (manufacturer's data). The tool consists of a 100 mm diameter (100) silicon wafer. The wafer has been etched to a depth of  $14 \pm 1$   $\mu\text{m}$  using a fluorine-based plasma by deep reactive ion etching. The tool is patterned with a set of test features including rectangles, squares, and other shapes. The features' widths vary from 3  $\mu\text{m}$  to more than 100  $\mu\text{m}$ , and their spacings vary from 0.1 times to 10 times their widths. An example of the tool features is shown in Figure 2.

The test process cycle begins when the part and tool are placed between the platens and heated to 120 °C. The platens are driven together at 10 mm/min until a threshold force is detected, indicating that the platens are in contact with the part and tool. The platens are then driven together at 5 mm/min until the desired embossing pressure of 4 MPa is reached. This pressure is maintained for 1 minute. The platens are then cooled to the de-molding temperature while the pressure is further maintained. When the de-molding temperature is reached, the platens are separated. The tool is separated from the part using tweezers and a razor blade. The part is then removed from the platens and allowed to cool to room temperature in air. In certain tests, the part is maintained at 120°C after the pressure is removed but prior to de-molding to investigate the evolution of shape recovery over time.

The parts produced in these tests have been measured using a Zygo NewView 5000 white-light profilometer. Selected parts were sputtered with 100 Å of gold and imaged with a FEI/Philips XL30 FEG ESEM.

## Results and Discussion

Our primary aim is to understand how the quality of embossed features depends on the temperature at which the tool is removed from the polymeric workpiece. Figure 3 shows cross-sections through 100  $\mu\text{m}$  wide square features within parts that were cooled under differing conditions. Conventionally, the polymeric workpiece is cooled from the forming temperature to well below  $T_g$

while in contact with the mold and under a compressive load. Under these conditions, a ridge of polymer has developed along one edge of the feature. This ridge is approximately 20  $\mu\text{m}$  wide and its height is of a similar magnitude to the depth of the embossed feature. Such ridges are undesirable because they make it harder to attach the surface of an embossed part to other materials. Moreover, substantial bending stresses are induced in the mold and part by the differential thermal contraction of the two materials; these stresses readily cause silicon tools to fracture. Figure 4 is a scanning electron micrograph of a cold-de-molded feature; it implies that the ridge was formed by the lateral compression of the polymer as it attempted to contract more than the mold during cooling.

If, instead of de-molding at 50 °C, we remove the compressive load from the part and tool while both are at 120 °C, immediately separate the tool from the part and then allow the part to cool, polymer ridges are not created. The final depths of the features, however, are about 10% smaller than in the cold-de-molding case, and the bases of the embossed features acquire an arched shape with a peak height of a few hundred nanometers. We attribute these distortions to the relaxation of elastic strain in the workpiece when the load is removed. Since the load is removed when the material is above its glass transition temperature, and thus its elastic modulus (as well as its viscosity) is substantially lowered, the amount of elastic strain relaxed is larger than if the load were removed at a lower temperature. Moreover, we expect the amount of elastic relaxation to be proportional to the pressure acting on the material just before de-molding, and the arched shapes of the feature bottoms are consonant with the center-high parabolic distribution of pressure that is developed when compressing a layer of viscous material [17]. Other possible causes of arching are adhesion of the mold to the hot polymer, and global warping of the sample.

If, however, we cool the part by 10–20 °C before unloading and de-molding, the features produced are of excellent quality. Edge ridges are not seen, the depths of the features are faithful to the dimensions of the mold, and there is no observable arching at the bottoms of the features. It therefore appears that the glass transition temperature of the PMMA used here lies between 110 and 120 °C: we believe that cooling the polymer to 110 °C or lower brings about an increase in its elastic modulus that is sufficient to eliminate appreciable shape spring-back. Yet, a temperature change under load of 10–20 °C does not seem to have induced damaging thermal stresses in the 50 mm wide square parts used here. Figure 5 illustrates the excellent replication seen in a part de-molded at 110 °C.

If it is desired to unload and de-mold the part while above the polymer's glass transition temperature — perhaps in order to reduce processing times — we need to consider how the embossed topography will evolve over

time after de-molding. Figure 6 shows cross-sections through 100  $\mu\text{m}$  wide square features that were all unloaded and de-molded at 120  $^{\circ}\text{C}$ , but which were subsequently allowed to sit, or “soak,” at 120  $^{\circ}\text{C}$  for varying periods of time before cooling. We see that as the nominal soaking time increases from zero to 10 minutes, the depths of the features reduce by up to 15%. The sidewalls of the features move apart, and the angle between them increases. The arching of the feature bottoms also appears to dissipate slightly after a 10-minute soak. Figure 7 illustrates the geometry of a 100  $\mu\text{m}$  wide channel subjected to a 10-minute soak at 120  $^{\circ}\text{C}$ . It should be noted that because cooling from 120  $^{\circ}\text{C}$  to room temperature takes approximately 3 minutes, even parts that start to be cooled immediately after de-molding experience some of the effects of soaking.

We have also investigated the evolution over time of groups of five embossed 30  $\mu\text{m}$  wide channels that are separated by 3  $\mu\text{m}$ . Figure 9a shows that when an embossing pressure of  $\sim 4.5$  MPa was applied for 2 minutes at 120  $^{\circ}\text{C}$  and de-molding was followed immediately by cooling, the 3  $\mu\text{m}$  wide walls between channels are not fully formed: they are approximately half as tall as the features on the mold. We can attribute this malformation to the incomplete transport of polymer into the narrow recesses of the mold, rather than to any relaxation of the topography immediately after unloading: even when de-molding occurs after cooling to 90  $^{\circ}\text{C}$ , the walls are of a similar height. If, however, the part is unloaded and de-molded at 120  $^{\circ}\text{C}$  and allowed to soak at that temperature for 5 minutes, the 3  $\mu\text{m}$  wide walls reduce in height by about 50% (Figure 8b). Meanwhile, the 100  $\mu\text{m}$  wide features contracted by only about 10% in 5 minutes (Figure 6). We interpret the faster re-flow of narrower features to show that surface tension is at least in part responsible for the viscous deformation of embossed structures during soaking.

## Conclusion

These preliminary experiments aimed to establish whether the hot embossing of thermoplastic polymers can be improved by unloading the polymeric workpiece at a higher temperature than is conventionally considered appropriate. It was found that minimizing the amount of cooling that is done under load can eliminate the formation of polymer ridges at feature edges, and reduces the propensity of silicon embossing tools to fracture during de-molding.

The best pattern fidelity was obtained by unloading and de-molding at a temperature slightly below the material’s glass transition (unloading at 90–110  $^{\circ}\text{C}$  in this case), although it is possible to unload and de-mold above the glass transition temperature and still obtain features whose dimensions deviate less than 10% from those on the mold. The depths of features on a mold used for hot

de-molding might be slightly increased to compensate for the subsequent contraction of features in the polymeric substrate.

Hot de-molding might be used to reduce processing times, and could prove necessary in reel-to-reel embossing systems. If de-molding occurs above the material’s glass transition, the part should be cooled as quickly as possible to minimize the distortion of parts. Soaking times in excess of three minutes at 120  $^{\circ}\text{C}$  lead to the appreciable distortion of features. Ideally, part cooling would happen within seconds of de-molding. Moreover, embossing apparatus that performs de-molding when the polymer is still soft will need to handle parts in such a way that they do not warp during their subsequent cooling.

Hot micro-embossing has great potential as a manufacturing technique for polymer-based microfluidic, micro-optical, and other devices with nanometer-scale and larger features. In the conventional HME process, production time is long because of the thermal cycle. Although the thermal cycle time can be reduced through novel heating methods and clever machine design, quality problems caused by thermal stress remain. High-temperature de-molding can improve feature quality at the same time as potentially reducing processing times by permitting heating and cooling of the part to occur separately from the embossing apparatus.

## Acknowledgements

We gratefully acknowledge the support of the Singapore-MIT Alliance. We further acknowledge helpful discussions with Aaron Mazzeo and Nici Ames and the support of the staff of the Microsystems Technology Laboratories at MIT.

## References

- [1] M. Hashimoto, F. Barany, and S. A. Soper, "Polymerase chain reaction/ligase detection reaction/hybridization assays using flow-through microfluidic devices for the detection of low-abundant DNA point mutations," *Biosensors and Bioelectronics*, vol. 21, pp. 1915-1923, 2006.
- [2] I. Frese, U. Schwab, E. Nahrstedt, T. Klotzbuecher, S. Kunz, U. Teubner, and T. Doll, "Polymer based optical interconnect components for high-speed Datacom approaches - Micromachining supported manufacturing," *Optics Communications*, vol. 265, pp. 434-440, 2006.
- [3] M. Hansen, D. Nilsson, D. M. Johansen, S. Balslev, and A. Kristensen, "A nanoimprinted polymer lab-on-a-chip with integrated optics," presented at *Advancements in Polymer Optics Design, Fabrication, and Materials*, San Diego, CA, USA, 2005.

- [4] C. Lu, Y.-J. Juang, L. J. Lee, D. Grewell, and A. Benatar, "Analysis of laser/IR-assisted microembossing," *Polymer Engineering and Science*, vol. 45, pp. 661-668, 2005.
- [5] C.-H. Chen, C.-P. Liu, Y.-C. Lee, F.-B. Hsiao, C.-Y. Chiu, M.-H. Chung, and M.-H. Chiang, "IR laser-assisted micro/nano-imprinting," *Journal of Micromechanics and Microengineering*, vol. 16, pp. 1463-7, 2006.
- [6] K. Seunarine, N. Gadegaard, M. O. Riehle, and C. D. W. Wilkinson, "Optical heating for short hot embossing cycle times," *Microelectronic Engineering*, vol. 83, pp. 859-63, 2006.
- [7] S.-J. Liu and Y.-T. Dung, "Hot embossing precise structure onto plastic plates by ultrasonic vibration," *Polymer Engineering and Science*, vol. 45, pp. 915-925, 2005.
- [8] M. Marcus and A. Benatar, "Experiments in ultrasonic micro-embossing of PMMA," presented at ANTEC 2006, May 7-11 2006, Charlotte, NC, United States, 2006.
- [9] T. E. Kimerling, W. Liu, B. H. Kim, and D. Yao, "Rapid hot embossing of polymer microfeatures," *Microsystem Technologies*, vol. 12, pp. 730-735, 2006.
- [10] J.-H. Chang and S.-Y. Yang, "Development of fluid-based heating and pressing systems for micro hot embossing," *Microsystem Technologies*, vol. 11, pp. 396-403, 2005.
- [11] D. Yao, A. Y. Yi, L. Li, and P. Nagarajan, "Two-station embossing process for rapid fabrication of polymer microstructures," presented at ANTEC 2006, May 7-11 2006, Charlotte, NC, United States, 2006.
- [12] M. Worgull and M. Hecke, "New aspects of simulation in hot embossing," *Microsystem Technologies*, vol. 10, pp. 432-437, 2004.
- [13] K. Hanada, Y. Hashiura, R. Maeda, T. Sano, and H. Negishi, "Micro-forming of PMMA for optical components," presented at AIEA 2002, 2-6 Dec. 2002 Sydney, NSW, Australia.
- [14] Y. Guo, G. Liu, Y. Xiong, and Y. Tian, "Study of the de-molding process—implications for thermal stress, adhesion and friction control," *Journal of Micromechanics and Microengineering*, vol. 17, pp. 9-19, 2007.
- [15] D. Yao and P. Nagarajan, "Cold forging method for polymer microfabrication," presented at ANTEC 2004, May 16-20 2004, Chicago, IL., United States, 2004.
- [16] M. Dirckx, "Design of a Fast Cycle Time Hot Micro-Embossing Machine," in *Mechanical Engineering*. Cambridge, MA: Massachusetts Institute of Technology, 2005.
- [17] R. Byron Bird, *Dynamics of Polymeric Liquids*, New York: Wiley, 1977.

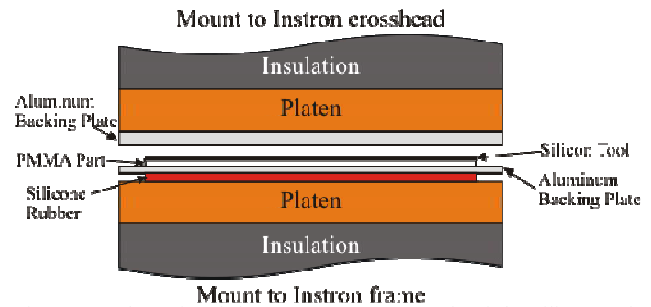


Figure 1. Schematic of the HME set-up. A stack of the silicon tool, PMMA workpiece, an aluminum backing plate and a soft silicone rubber layer are compressed between heated platens.

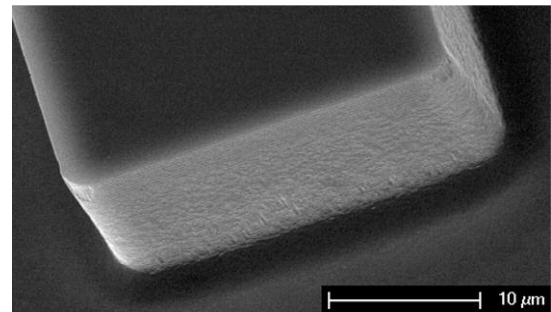


Figure 2. 30  $\mu\text{m}$  wide and 15  $\mu\text{m}$  tall feature on the silicon tool. The fine "scalloping" on the sidewalls is an artifact of the plasma etching process used. The trench surrounding the base of the feature is caused by the deflection of ions from the sidewalls of the feature during etching.

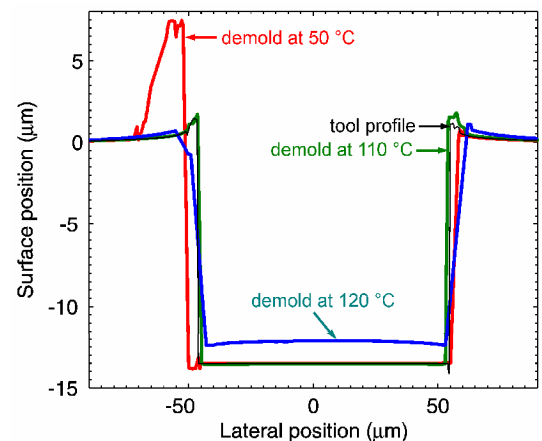


Figure 3. Profiles of a 100  $\mu\text{m}$  wide square feature from parts de-molded at varying temperatures. The ridge apparent in the 50  $^{\circ}\text{C}$  part is attributed to material ploughed up by differential thermal contraction of mold and substrate.

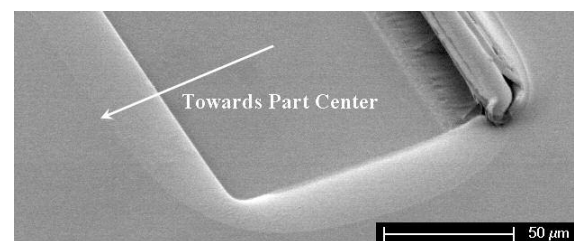


Figure 4. End of a 100  $\mu\text{m}$  wide channel in a part that was de-molded at 50  $^{\circ}\text{C}$ . Note the severe distortion of the material that experienced compressive stress during the differential thermal contraction of tool and part.

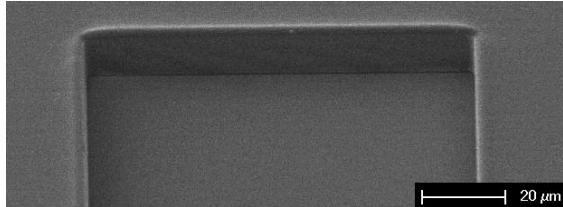


Figure 5. End of a 100  $\mu\text{m}$  wide channel from a part that was de-molded at 110  $^{\circ}\text{C}$ . Note the “lip” along the top of the channel corresponding to the groove at the base of the tool’s feature, indicating that the material has fully conformed to the tool.

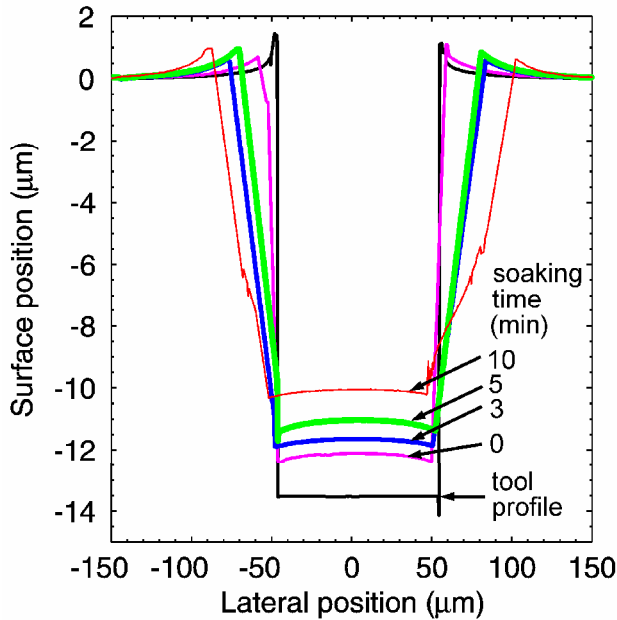


Figure 6. Profiles of 100  $\mu\text{m}$  wide square features on embossed parts that were “soaked” at elevated temperatures after releasing the forming pressure, but before de-molding.

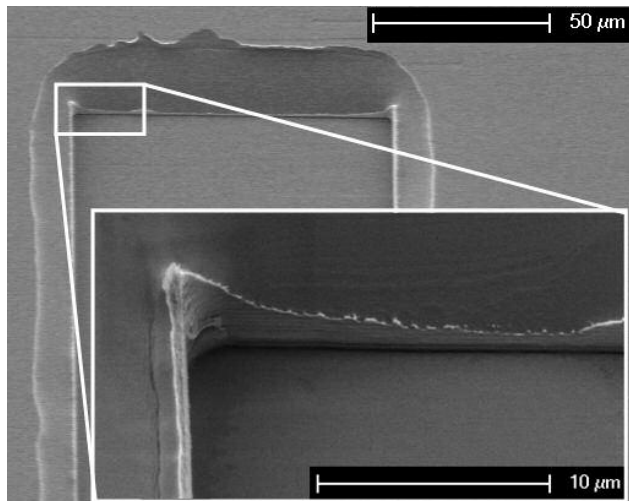


Figure 7. End of a 100  $\mu\text{m}$  wide channel from a part that was held at 120  $^{\circ}\text{C}$  for 10 min after removing the pressure. Inset showing wall surface texture. The RIE scallops have been replicated, as has the “lip” along the edge. The material formerly in contact with the base of the tool feature has relaxed by several micrometers.

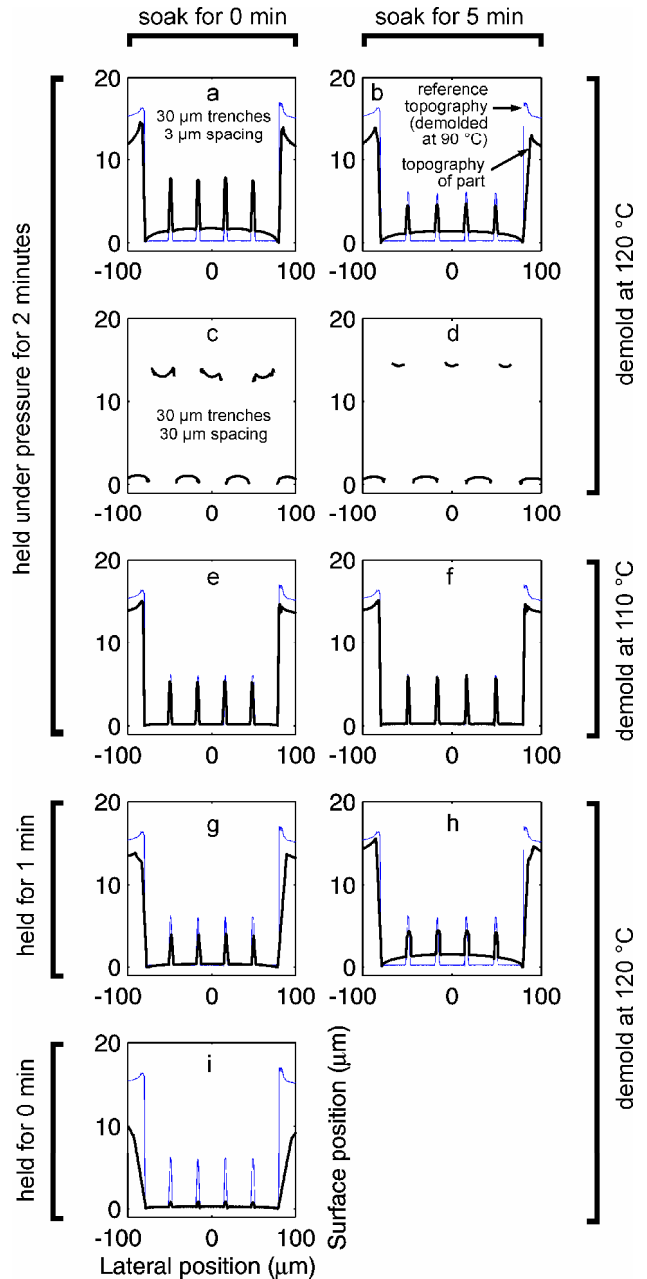


Figure 8. The relaxation of sub-100  $\mu\text{m}$  embossed topographies after demolding. (a) and (b) show 3  $\mu\text{m}$  wide walls formed at 4.5 MPa, before and after a 5-minute soak at 120  $^{\circ}\text{C}$ . (c) and (d) show that 30  $\mu\text{m}$ -wide walls between trenches are fully formed after 4.5 MPa is applied for 2 minutes. (e) and (f) indicate that re-flow of 3  $\mu\text{m}$  wide walls is minimal if de-molding occurs at 110  $^{\circ}\text{C}$ . (g) and (h) show that 3  $\mu\text{m}$  wide walls are less well formed after the embossing pressure is applied for 1 minute instead of 2 minutes, and suggest that post-de-molding re-flow is less substantial after holding for one minute than after holding for two minutes. (i) shows that small features barely begin to be formed if the pressure is applied for much less than one minute.

Key Words: Hot embossing, De-molding, Cycle time, Quality